

1H-Indene과 Mono-sila-1H-Indene의 구조와 방향족성에 대한 이론적 연구

Reza Ghiasi* and Majid Monnajemi†

Department of Chemistry, East Tehran Branch (Ghiam Dasht), Islamic Azad University, Tehran, IRAN

†Science and Research Branch, Islamic Azad University, Tehran, IRAN

(2006. 6. 29 접수)

Theoretical Studies on the Structure and Aromaticity of 1H-Indene and Mono-sila-1H-Indene

Reza Ghiasi* and Majid Monnajemi†

Department of Chemistry, East Tehran Branch (Ghiam Dasht), Islamic Azad University, Tehran, IRAN

†Science and Research Branch, Islamic Azad University, Tehran, IRAN

(Received June 29, 2006)

요 약. Hybrid DFT 계산 방법을 이용하여 1H-Indene과 Mono-sila-1H-indene 분자의 구조와 특성에 관한 이론적 연구를 수행하였다. 이 분자들의 방향족성 특성 연구를 위하여 MO, 비등방성 자기 민감도 등을 계산하였다. 1H-Indene과 Mono-sila-1H-indene 분자들에 대한 X8-X9 결합의 상대적인 안정도와 특성을 이해하기 위하여 NBO 계산을 수행하였다. 그 결과, 8, 9 위치의 Si 원자들이 C 원자들로 치환되었을 때, p orbital의 기여도가 증가하였다. 이러한 결과는 X8-X9 결합 길이는 하이브리드 오비탈의 p 오비탈 기여도에 크게 영향받는 사실을 보여준다. NBO계산을 통하여 σ_{X8-X9} 로부터 σ^*_{X8-X9} 결합 오비탈로의 비편재화에 기인하는 정량적인 에너지 안정화 세기를 결정하였다. MO 분석 결과 연구 대상 분자들의 방향족성은 3개의 비편재화된 pMO와 2개의 비편재화된 sMO에 의해서 주로 영향 받는다는 사실을 알 수 있었다.

주제어: 1H-Indene, Sila-1H-Indene, Aromaticity, magnetic properties, Natural bond orbital (NBO)

ABSTRACT. The electronic structure and properties of the 1H-indene and mono-sila-1H-indene series have been investigated using basis set of 6-31G(d, p) and hybrid density functional theory. Basic measures of aromatic character derived from structure, molecular orbitals, a variety of magnetic criteria (magnetic isotropic and anisotropic susceptibilities) are considered. Energetic criteria suggest that **In(Si7)** enjoy conspicuous stabilization. However, by magnetic susceptibility isotropic this system are among the least aromatic of the family: Within their isomer series, **In(Si4)** is the most aromatic using this criteria. Natural bond orbital (NBO) analysis method was performed for the investigation of the relative stability and the nature of the 8-9 bonds in 1H-indene and mono-sila-1H-indene compounds. The results explained that how the p character of natural atomic hybrid orbital on X8 and X9 (central bond) is increased by the substitution of the C8 and C9 by Si. Actually, the results suggested that in these compounds, the X8-X9 bond lengths are closely controlled by the p character of these hybrid orbitals and also by the nature of C-Si bonds. The magnitude of the molecular stabilization energy associated to delocalization from σ_{X8-X9} and to σ^*_{X8-X9} bond orbital were also quantitatively determined. Molecular orbital (MO) analysis further reveal that all structure has three delocalized π MOs and two delocalized σ MOs and therefore exhibit the aromaticity.

Keywords: 1H-Indene, Sila-1H-Indene, Aromaticity, magnetic properties, Natural bond orbital (NBO)

INTRODUCTION

The relatively weak σ -bonding ability of silicon versus carbon results in interesting structural and electronic features within the framework of sila-1H-indene compounds. This substantial difference in σ -bonding for silicon versus carbon may well be the feature that limits the successful synthesis and isolation of these potentially aromatic silaorganic compounds and establishes them as challenges for computational organosilicon chemistry.¹ Much attention has been focused on the chemistry of sila-aromatic compounds, i.e. Si-containing $[4n+2]\pi$ ring systems and a number of reports on the formation and reactions of transient silaaromatics. The lack of experimental information on the structure and bonding nature of these compounds necessitates the theoretical studies on these species. Although some of these species were characterized spectroscopically in low-temperature matrices no isolation of sila-aromatic compounds has been reported due to their high reactivity.

Indene and its heterocyclic analogs have wide and important biological and industrial applications.² The theoretical and experimental literature comparing indene is fairly substantial, and its theoretical aspects in general have recently been critically studied.³⁻⁵ From these examinations one sees that the actual experimental knowledge concerning sila-aromatic compounds is still relatively scant due to the elusive nature of such compounds.

1H-indene was investigated before computationally. S. Zilberg et al. studied the low-lying electronic states of indene⁵. A.A. El-Azhary⁶ reported DFT study of the geometries and vibrational spectra of indene and some of its heterocyclic analogues, benzofuran, benzoxazole, bensothiophene, benzothiazole, indole and indazole. The focus of this work is on the theoretical studies of mono-sila-1H-indene. The present study investigates structure, bond characterization and aromaticity of the indene, and mono-silaindene compounds.

Aromaticity is an important concept in organic chemistry; it explains the structural stability and chemical reactivity of molecules.⁷⁻¹³ The common

character of these molecules with aromaticity is that these molecules are planar with delocalized π orbitals. Recent studies extended the concepts of aromaticity to organometallic¹⁴⁻¹⁹ and all metal²⁰⁻²⁴ systems. It was found that not only π bond but also σ bond has electron delocalization. For the sake of quantitative analysis, some criteria such as structural (geometric), energetic, magnetic, and reactivity related ones were proposed for the aromaticity study. Which one is the best criterion for aromaticity is still in debate.²⁵⁻³¹

COMPUTATIONAL METHODS

All calculations were carried out with the Gaussian 98 suite of program³² using the 6-31G(d, p) basis set for all elements (C, H, Si).³³ Geometry optimization were performed utilizing Becke's hybrid three-parameter exchange functional and the nonlocal correlation functional of Lee, Yang, and Parr (B3LYP)^{34,35}. A vibrational analysis was performed at each stationary point found, that confirm its identity as an energy minimum. The molecular orbital (MO) calculations were performed at B3LYP/6-31G(d, p) level. Atomic charges were calculated with the natural bond orbital (NBO) program³² implemented in the G98 package, using B3LYP/6-31G(d, p).

The magnetic susceptibility were computed using continues set gauge transformations, CSGT^{36,37}, methods also using the 6-31G(d, p) basis set.

RESULTS AND DISCUSSION

Relative Energetics and Vibrational frequencies

Relative energies at B3LYP level of theory are reported in *Table 1*. The order of the stability of mono-sila-1H-indenes is: **In(Si7)** (0.0) > **In(Si6)** (19.70) > **In(Si2)** (22.11) > **In(Si3)** (22.48 kcal/mol) > **In(Si4)** (23.13 kcal/mol) > **In(Si1)** (23.41 kcal/mol) > **In(Si5)** (23.86 kcal/mol) > **In(Si8)** (29.53) > **In(Si9)** (31.00 kcal/mol).

The calculated lowest harmonic frequencies are given in *Table 1*. The lowest vibrational frequencies calculated for all structure are larger enough to prove the minimum.

Table 1. Relative energies (kcal/mol) and Low frequencies (cm^{-1}) for 1H-indene and various mono-sila-1H-indenes at B3LYP/6-31G** level of theory

Structure	E (Hartree)	ΔE (kCal/mol)	Lowest frequencies (cm^{-1})
1H-indene	-347.775	-	197.7
In(Si1)	-599.123	23.41	172.3
In(Si2)	-599.125	22.11	164.0
In(Si3)	-599.124	22.48	170.8
In(Si4)	-599.123	23.13	162.3
In(Si5)	-599.122	23.86	156.8
In(Si6)	-599.129	19.70	75.7
In(Si7)	-599.160	0.00	150.4
In(Si8)	-599.113	29.53	73.5
In(Si9)	-599.111	31.00	118.7

Structure

There are experimental microwave³⁸ and electron diffraction³⁹ geometries reported for 1H-indene. Since the experimental geometries determined by microwave spectroscopy are usually more accurate than those determined by electron diffraction or X-Ray spectroscopy, the microwave experimental geometries of 1H-indene are included in Table 2. We didn't find experimental geometries reported for mono-sila-1H-indene series in the literature.

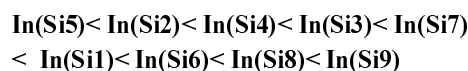
The data in Table 2 show that the B3LYP-predicted bond lengths are about 0.01-0.02 Å, too short from the experimental bond lengths. A summary of structural parameters for the whole set of sila-aromatic compounds is presented in Fig. 1. In the present study, one sees a convergence of structural

parameters toward a SiC bond length of 1.77 Å. This value is about 0.01 Å below the corresponding average of double and single bond prototype systems (Fig. 1, Table 2). This is indicative of structural aromaticity analogous to that seen in 1H-indene.

In mono-sila-1H-indenes, calculations show that Si-C, C-C bonds of six members ring are delocalized because, these bonds length are below average of double and single bond prototype systems. These bonds in five members ring display single and double bond character.

Dipole moments and electric polarizabilities

Values of electric dipole moment of the 1H-indene and sila-1H-indenes, listed in Table 3. This table shows that values increase in the following order:



Polarizability is a measure of ability of a molecule to respond to an external electric field. When electrons of the molecules are subjected to an electric field, they acquire enough energy and can move along the direction of the applied field, thus, electric conductivity will take place. Diagonal elements of electric polarizability tensor (α_{xx} , α_{yy} , α_{zz}) have been calculated and reported in Table 3. These values show that polarizability is more for sila-1H-Indene species. The order of increasing α_{xx} , α_{yy} , α_{zz} in various isomers is:

Table 2. Structural parameters (Å) for Prototype Molecules

Prototype	Bond	Length(Å)
H ₂ SiCH ₂	Si=C	1.710 (1.799) ^a
H ₃ SiCH ₃	Si-C	1.888
C ₂ H ₄	C=C	1.330 (1.430)
C ₂ H ₆	C-C	1.530
		C1-C2: 1.401 [1.381] ^b ; C2-C3: 1.397 [1.383]
		C3-C4: 1.397 [1.406]; C4-C9: 1.396 [1.408]
		C9-C5: 1.466 [1.484]; C5-C6: 1.347 [1.342]
		C6-C7: 1.511 [1.492]; C7-C8: 1.512 [1.468]
		C8-C9: 1.412 [1.410]; C8-C1: 1.388 [1.438]
C ₉ H ₈	CC	

^aThe values in parenthesis are average of single and double bonds.

^bThe values in bracket are by microwave spectroscopy. Other parameters are calculated at B3LYP/6-31G** level of theory.

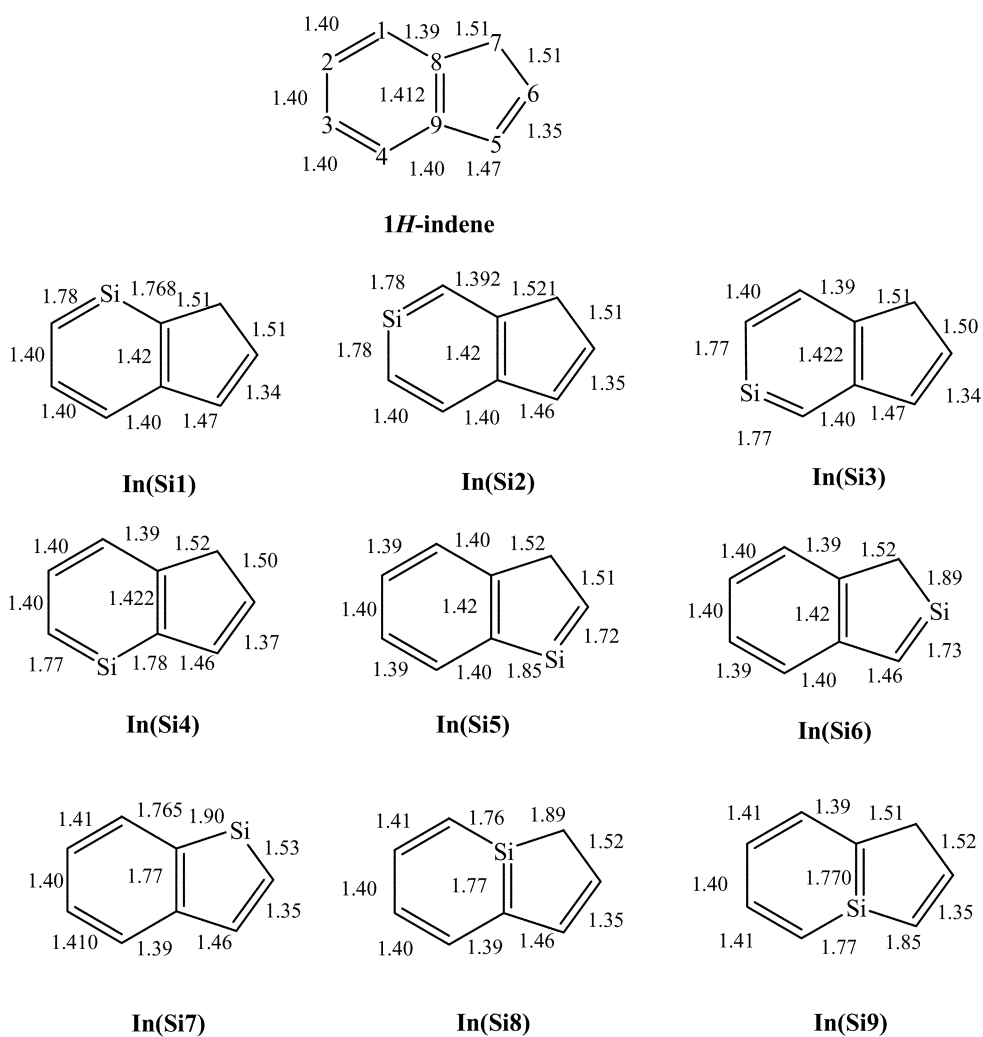
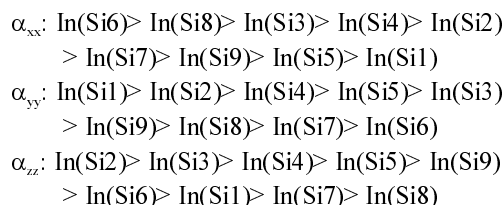


Fig. 1. Structures and bonds length (in Å) of 1H-indene and sila-1H-indenes.

Table 3. Polarizability tensor elements, and Dipole moment (Debye) for 1-H-indene and various mono-sila1-H-indenes at B3LYP/6-31G** level of theory

Structure	α_{xx}	α_{yy}	α_{zz}	Dipole moment (Debye):
1H-indene	121.2	103.4	36.3	0.7
In(Si1)	135.3	130.9	51.7	0.9
In(Si2)	145.8	129.3	52.7	0.5
In(Si3)	149.0	120.2	52.6	0.6
In(Si4)	147.9	123.1	52.4	0.6
In(Si5)	139.9	121.2	52.2	0.3
In(Si6)	171.3	107.4	51.8	1.4
In(Si7)	145.4	110.0	46.8	0.7
In(Si8)	150.2	116.6	51.3	1.4
In(Si9)	143.2	118.9	52.1	1.5

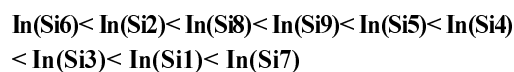


Macroscopic electric conductivity is proportional with molecular electric polarizability, therefore the electric conductivity increases in sila-1H-Indene species.

The HOMO–LUMO energy gaps

It is already known that orbital energy gaps from Koopman's theorem are overestimated since electron correlation is not included in the Hartree–Fock formalism and, furthermore, the electron density relaxation following to the excitation is not taken into account. Even though several difficulties can be pointed out in getting energy gaps from Koopman's theorem, its simplicity and no additional computational cost make it very attractive and an interesting approach to study larger and complex systems.

In a first approximation, the barrier for electron transfer is proportional to ΔE (HOMO–LUMO energy gap) value. Therefore, from the calculated ΔE values reported in *Table 4*, one can conclude that the molar contributions of sila-1-H-indene compounds to the bulk electric conductance are less than 1-H-indene. This trend in sila-1-H-indene compounds is:

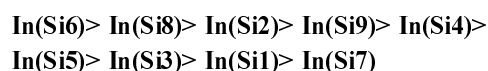


Absolute chemical hardness (η) has been used as a measure of kinetic stability or the reactivity of organic compounds. Within Koopman's approximation, hardness (η) is defined as half of the magnitude of the energy difference between the HOMO and LUMO^{40, 41}.

$$\eta = \frac{(\epsilon_{\text{LUMO}} - \epsilon_{\text{HOMO}})}{2} \quad (1)$$

The frontier orbital energies and the hardness of germatropylium computed at the B3LYP/6-31G(d, p) level are given in the *Table 4*. While the thermodynamic stabilities of the compounds under study are controlled by the skeleton of their structure, the kinetic stability seems to be dictated by the bonding type of the Si atom. **In(Si7)**, where the Si occupies the sp^3 center, are kinetically more stable than the other isomers. Whereas, in other structures are more reactive, in all these cases Si is tri-coordinated. So kinetic stability exactly follows the following order: isomers containing tetra-coordinated Si > isomers containing tri-coordinated. The relative stability and hardness values don't have a linear relationship.

Table 4 shows that, the ϵ_{HOMO} values of sila-1-H-Indenes are more than indene. The ϵ_{HOMO} of sila-1-H-Indenes decreases with the following trend:



An increase in the HOMO energy level shows better donors and their nucleophilicity increases.

Table 4. Frontier orbital energies (ϵ_{HOMO} and ϵ_{LUMO}), absolute chemical hardness (η) for 1-H-indene and various mono-sila-1-H-indenes at B3LYP/6-31G** level of theory

Structure	ϵ_{HOMO}	ϵ_{LUMO}	ΔE	$\eta = (\epsilon_{\text{HOMO}} - \epsilon_{\text{LUMO}})/2$
1H-indene	-0.212	-0.018	0.194	2.64
In(Si1)	-0.202	-0.027	0.175	5.50
In(Si2)	-0.189	-0.033	0.157	5.15
In(Si3)	-0.200	-0.029	0.171	5.43
In(Si4)	-0.195	-0.031	0.164	5.31
In(Si5)	-0.198	-0.035	0.163	5.39
In(Si6)	-0.187	-0.045	0.142	5.09
In(Si7)	-0.224	-0.046	0.178	6.09
In(Si8)	-0.189	-0.029	0.160	5.13
In(Si9)	-0.191	-0.031	0.160	5.20

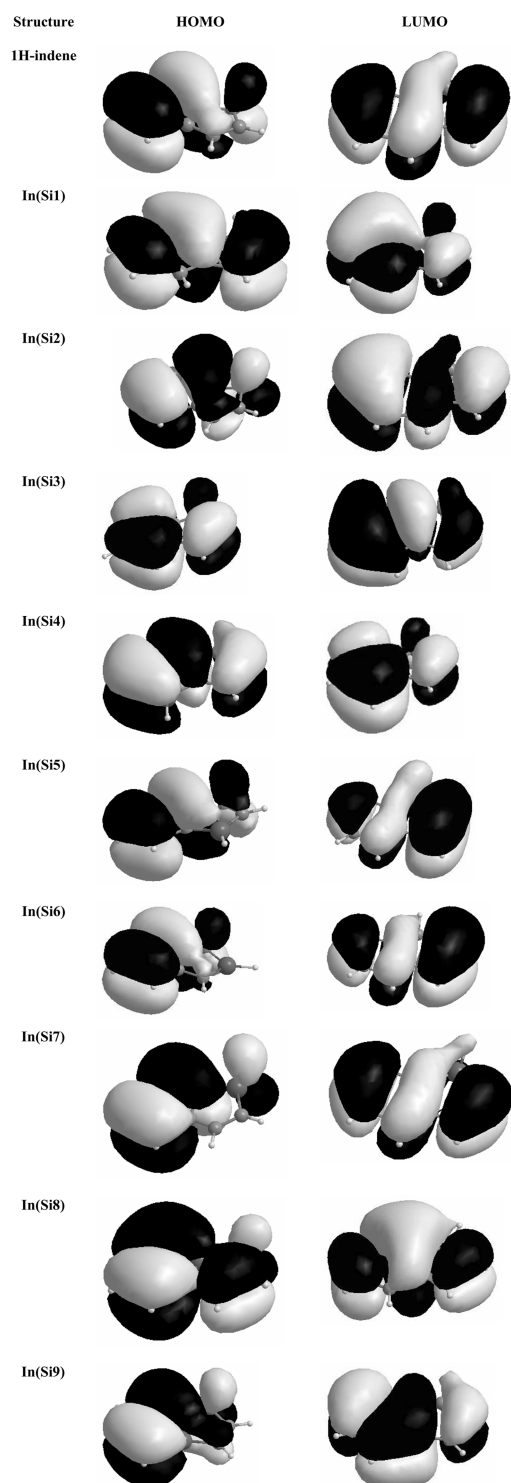
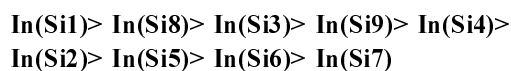


Fig. 2. Frontier molecular orbitals of 1H-indene and sila-1H-indenes.

On the other hand, the ϵ_{LUMO} values in sila-1-H-Indenes are less than indene. the ϵ_{LUMO} of sila-1-H-Indenes decreases with the following trend:



Electron accepting nature of isomers decreases with increasing of ϵ_{LUMO} .

The HOMOs and LUMOs of 1H-indene and sila-1H-indenes are shown in Fig. 2. Calculations illustrate HOMO and HOMO-1 are two π -bonding, which are mainly composed of the out-of-plane p ($2p_c$ or $3p_{si}$) orbital. HOMO-2 and HOMO-3 are two multicentered centripetal σ orbitals, which are comprised mainly of the 2s and p ($2p_c$ or $3p_{si}$) orbital in-ring plane. All together, there are three π -bonding MOs and two multicentered σ MOs that give the agreement with the famous $(4n+2)$ Hückel rule and render 1H-indene and sila-1H-indenes aromatic.

Magnetic Properties

Magnetic properties, including magnetic shieldings, magnetic susceptibilities, χ_M , magnetic susceptibility anisotropies, χ_{aniso} , have been computed for the set of sila-aromatic compounds and are summarized in Table 5. The magnetic susceptibility tensor describes the quadratic response of a molecule to an external magnetic field, and as such its isotropic and anisotropic components are relevant quantities to consider for the types of molecules studied

Table 5. B3LYP/6-31G** computed magnetic properties (ppm) related to aromaticity for 1-H-indene and various monosila-1-H-indenes using CSGT method

Structure	Isotropic	Anisotropic
1H-indene	-68.6751	44.6042
In(Si1)	-72.0508	43.9686
In(Si2)	-71.6618	42.7658
In(Si3)	-71.7316	43.2906
In(Si4)	-72.1955	43.1947
In(Si5)	-72.8792	44.7249
In(Si6)	-71.6827	42.6307
In(Si7)	-63.0494	41.0809
In(Si8)	-71.0642	48.2958
In(Si9)	-72.0055	51.1810

here. χ_{aniso} is a character of planar aromatic systems. The component of magnetic susceptibility tensor corresponding to the normal axis with respect to the ring is also affected by ring currents. A large negative anisotropy is observed for aromatic compounds; the converse is observed for antiaromatic systems.

For mono-sila-1H-indene χ_{aniso} predict the aromaticity ordering: **In(Si7) > In(Si6) > In(Si2) In(Si4) > In(Si3) > In(Si1) > In(Si5) > In(Si8) > In(Si9)**, albeit χ_{iso} predicts **In(Si5) > In(Si4) > In(Si1) > In(Si9) > In(Si3) > In(Si6) > In(Si2) > In(Si8) > In(Si7)**.

Minor variations aside, χ_{aniso} magnetic criteria agree on one thing: the isomer that is energetically the most stable (that is, **In(Si7)**) to be the most "aromatic" by energetic criteria.

NBO

Character of natural atomic hybrid orbital on C8 and C9

It seems useful to recall, briefly, some aspects concerning the concept and definition of NAO and natural hybrid orbital (NHO)⁴². A NAO is defined as a valence-shell atomic orbital derived from the diagonalization of the localized block of the full density matrix of a given molecule, associated with basis functions $\chi_i(A)$ on that atom, and fulfilling the simultaneous requirement of orthonormality and maximum occupancy. Although in an isolated atom, NAOs coincide simply with natural orbitals, in polyatomic molecule (in contrast to natural orbitals that become delocalized over all nuclear centers); the NAOs mostly retain one-center character. Consequently, NAOs are considered optimal for describing the molecular electron density around one-center in polyatomic molecules. Also, a NHO result from a symmetrically orthogonalized directed hybrid orbital derived through unitary transformation of NAO centered on a particular atom. Finally, according to the simple bond orbital picture, a NBO is defined as an orbital formed from NHOs. Therefore, for a localized s-bond between atoms A and B, the NBO is defined as

$$\sigma_{AB} = c_A h_A + c_B h_B \quad (2)$$

Table 6. Calculated natural hybrids (NHOs) on X8 and x9 positions and the polarization coefficient (c_A) of each hybrid in the corresponding NBO

Structure	X8-X9
1H-indene	σ : 0.7051 C 8 sp 2.12+0.7091 C 9 sp 2.15
In(Si1)	σ : 0.7063 C 8 sp 2.06+0.7079 C 9 sp 2.04 π : 0.7465 C 8 p 1.00+0.6654 C 9 p 1.00
In(Si2)	σ : 0.7066 C 8 sp 2.06+0.7077 C 9 sp 2.08
In(Si3)	σ : 0.7037* C 8 sp 2.04+ 0.7105 C 9 sp 2.08
In(Si4)	σ : 0.7038 C 8 sp 2.03+0.7104 C 9 sp 2.09
In(Si5)	σ : 0.7050 C 8 sp 2.01+0.7092 C 9 sp 1.98 π : 0.6818 C 8 p 1.00+0.7316 C 9 sp 1.00
In(Si6)	σ : 0.7046 C 8 sp 2.01+0.7096 C 9 sp 2.08
In(Si7)	σ : 0.7035 C 8 sp 2.06+0.7107 C 9 sp 2.03
In(Si8)	σ : 0.5121Si 8 sp 2.29+0.8589 C 9 sp 2.41
In(Si9)	σ : 0.8579 C 8 sp 2.31+0.5138 Si 9 sp 2.27

where h_A and h_B are the natural hybrids centered on atoms A and B. NBOs closely correspond to the picture of localized bonds and lone pairs as basic units of molecular structure, so, that is possible to conveniently interpret ab initio wave functions in terms of the classical Lewis structure concepts by transforming these functions to NBO form. Table 6 presents the resulted natural atomic hybrids h_A on 8 and 9 positions with the polarization coefficient c_A for each hybrid in the corresponding NBO. The inspection of the results reported in Table 6 reveals that:

(a) As C8 (or C9) is (are) replaced by Si the p character of C9 (or C10) NHO of σ 8-9 bond orbital increases.

(b) When other carbon atoms are replaced by Si, the p character of decreases. Moreover, the p character of 8 and 9 atoms NHO of σ 8-9 in these compounds is less than the p character of carbon NHO of σ 8-9 in 1H-indene. Therefore, the results suggest in these compounds, the 8-9 bond lengths are essentially controlled by the p character of these hybrid orbitals and also by the nature of the C-Si bonds.

(c) In all molecules the natural hybrids (NHOs) on C8 and C9 positions show that σ contribute in bond, but in **In(Si1)** and **In(Si1)** show that σ bonding and π bonding contribute in bond.

Identify principle delocalizing acceptor orbitals

associate with each donor NBO and their topological relationship to this NBO, i.e., whether attached to the same atom (geminal), to an adjacent bonded atom (vicinal) or to a more remote site, is possible. These acceptor NBOs will generally correspond to the principle delocalization tails of the non Lewis molecular orbital (NLMO) associated with the parent donor NBO.

Donor–acceptor (bond–antibond) interactions

In the NBO analysis, in order to complete the span of the valence space, each valence bonding NBO (σ_{AB}), must in turn, be paired with a corresponding valence antibonding NBO (σ^*AB)

$$\sigma^*_{AB} = c_A h_A - c_B h_B \quad (3)$$

Namely, the ‘Lewis’-type (donor) NBOs are complemented by the ‘non-Lewis’-type (acceptor) NBOs that are formally empty in an idealized Lewis structure picture. Readily, the general transformation to NBOs leads to orbitals that are unoccupied in the formal Lewis structure. As a result, the filled NBOs of the natural Lewis structure are well adapted to describe covalency effects in molecules. Since the non-covalent delocalization effects are associated with $\sigma \rightarrow \sigma^*$ interactions between filled (donor) and unfilled (acceptor) orbitals, it is natural to describe them as being of ‘donor–acceptor’, charge transfer, or generalized ‘Lewis base–Lewis acid’ type. The antibonds represent unused valence-shell capacity and spanning portions of the atomic valence space

that are formally unsaturated by covalent bond formation. Weak occupancies of the valence antibonds signal irreducible departures from an idealized localized Lewis picture, i.e. true ‘delocalization effects’. As a result, in the NBO analysis, the donor–acceptor (bond–antibond) interactions are taken into consideration by examining all possible interactions between ‘filled’ (donor) Lewis-type NBOs and ‘empty’ (acceptor) non-Lewis NBOs and then estimating their energies by second-order perturbation theory. These interactions (or energetic stabilizations) are referred to as ‘delocalization’ corrections to the zeroth-order natural Lewis structure. For each donor NBO (i) and acceptor NBO (j), the stabilization energy E associated with $i \rightarrow j$ delocalization, is explicitly estimated by the following equation:

$$E = \Delta E_{ij} = q_i \frac{F^2(i,j)}{\epsilon_j - \epsilon_i} \quad (4)$$

Where q_i is the i th donor orbital occupancy, ϵ_i ; ϵ_j are diagonal elements (orbital energies) and $F(i,j)$ off diagonal element, respectively associated with NBO Fock matrix. Therefore, consideration of the valence antibond (σ^*) leads to a far-reaching extension of the elementary Lewis structure concept, by achieving delocalization corrections in simple NBO perturbative estimates by using Eq 4. *Table 7* shows the interactions that give the strongest stabilization.

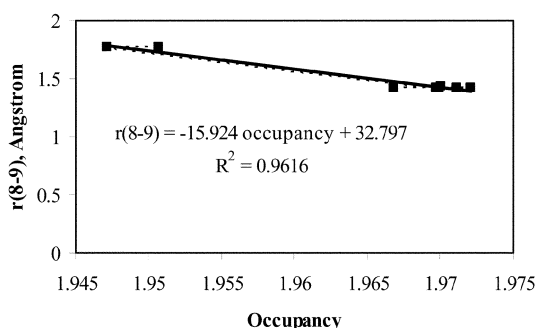
The Lewis NBOs in *Table 8* describes valence non-Lewis, Rydberg non-Lewis, $\sigma C8C9$ and $\sigma^* C8C9$ bond orbital occupancies.

Table 7. Stabilization energies (in kcal/mol) associated with delocalizations from $\sigma C8C9$ bond orbital and delocalizations to $\sigma^* C8C9$ bond orbital, represented by ($\sigma \rightarrow$) and ($\rightarrow \sigma^*$), respectively

Structure	$\rightarrow \sigma^* 8-9$				$\sigma 8-9 \rightarrow$	
	$\sigma 1-8$	$\sigma 8-7$	$\sigma 9-4$	$\sigma 9-5$	$\sigma^* 1-8$	$\sigma^* 9-4$
IH-indene	3.82	1.54	4.00	1.96	3.56	3.73
In(Si1)	2.16	2.34	4.25	2.07	2.22	4.49
In(Si2)	4.55	1.29	4.09	1.92	3.82	3.77
In(Si3)	3.97	1.46	4.82	1.70	3.64	4.05
In(Si4)	4.03	1.60	2.22	2.85	4.21	2.23
In(Si5)	3.95	1.77	4.43	0.63	3.48	3.82
In(Si6)	3.66	1.71	3.59	2.68	3.44	3.31
In(Si7)	3.88	0.83	4.11	2.03	3.39	3.83
In(Si8)	2.65	3.02	2.28	1.34	1.25	2.91
In(Si9)	2.27	1.09	2.54	2.76	2.97	1.14

Table 8. Calculated valence non-Lewis, Rydberg non-Lewis, σ C8C9 and σ^* C8C9 bond orbital occupancies.

Structure	Valence non-Lewis	Rydberg non-Lewis	σ 8-9	σ^* 8-9
1H-indene	1.43012	0.08786	1.96684	0.02770
In(Si1)	1.45687	0.08847	1.97215	0.02480
In(Si2)	1.44674	0.08753	1.96995	0.03084
In(Si3)	1.44020	0.08785	1.96980	0.03067
In(Si4)	1.45315	0.08823	1.97210	0.02490
In(Si5)	1.43574	0.08981	1.97109	0.02562
In(Si6)	1.48454	0.08764	1.97004	0.03204
In(Si7)	1.40340	0.09364	1.96971	0.02648
In(Si8)	1.42161	0.09659	1.94713	0.03204
In(Si9)	1.40014	0.09836	1.95066	0.02928

Fig. 3. The linear trend of σ 8-9 occupancy versus 8-9 bond length of 1H-indene and sila-1H-indenes.

The results reported in Table 8, show also that for σ 8-9 bond orbital, the maximum occupancy is obtained for **In(Si1)** and the minimum occupancy results for **In(Si8)**. On other hand, for σ^* 8-9 bond orbital, the maximum occupancy is obtained for **In(Si8)**, **In(Si6)** and the minimum occupancy is found for **In(Si1)**.

Fig. 3 illustrates also the linear trend of σ 8-9 occupancy versus 8-9 bond length. For example, the 8-9 bond lengths in **In(Si8)** is lowest, similarly the σ 8-9 occupancies in compound **In(Si1)** is also most than other.

$$r(8-9) = -15.924 \text{ occupancy} + 32.797; R^2 = 0.9616$$

CONCLUSIONS

In the present article, we have described the electronic structure and properties of the 1H-indene and sila-1H-indene as given by density functional method.

Basic measures of aromatic character, such as those gauged from assessment of structure, and molecular orbitals are reported in addition to new magnetic properties. Comparing structural, energetic, and magnetic effects in 1H-indene with those in mono-silaaromatic compounds, several points are noted. First, energetics, structural parameters, and orbital structures (including partial charges) effectively provide insight in electron delocalization tendencies.

The results concerning the application of NBO method for the investigation of the relative stability and the nature of the X8-X9 central bond in indene and sila-1H-indene were reported.

REFERENCES

1. Patai, S.; Rappoport, Z.; Eds, *The Chemistry of Organic Silicon Compounds*; Wiley: New York, 1989; p 1015.
2. (a) Katritzky, A. R.; Rees, C. W.; Scriven, E. F. (Editors-in-Chief) *Comprehensive Heterocyclic Chemistry, A review of the Literature 1982–1995. The Structure, Reactions, Synthesis and Uses of Heterocyclic Compounds*, Pergamon Press, UK, 1996. (b) Barton, D.; Ollis, W.D. *Comprehensive Organic Chemistry: The Synthesis and Reactions of Organic Compounds*, Pergamon Press, New York, 1979.
3. Andrés L. S.; Borin, A. C. *Chemical Physics*. **2000**, *26*, 267.
4. Klots, T. D. *Spectrochimica Acta Part A: Molecular and Biomolecular Spectroscopy*, **1995**, *51*, 2307.
5. Zilberg, S.; Kandler, S.; Haas, Y. *J. Phys. Chem.* **1996**, *100*, 10869.
6. A. A. El-Azhary, *Spectrochimica Acta Part A: Molecular and Biomolecular Spectroscopy*. **1999**, *55*, 2437.

7. Collins, J. B.; Schleyer, P. v. R. *Inorg. Chem.* **1977**, *16*, 152.
8. Jemmis, E. D.; Alexandratos, S.; Schleyer, P. v. R.; Streitwieser, A.; Schaefer, H. F. *J. Am. Chem. Soc.* **1978**, *100*, 5695.
9. Krogh-Jespersen, K.; Chandrasekhar, J.; Schleyer, P. v. R. *J. Org. Chem.* **1980**, *45*, 1608.
10. Garrat, P. J. *Aromaticity*; Wiley: New York, 1986.
11. Minkin, V. J.; Glukhovesev, M. N.; Simkin, B. Y. *Aromaticity and Antiaromaticity: Electronic and Structural Aspects*; Wiley: New York, 1984.
12. Schleyer, P. v. R.; Jiao, H. *Pure Appl. Chem.* **1996**, *68*, 209.
13. Krygowski, T. M.; Cvranski, M. K.; Czarnocki, Z.; Hafelinger, G.; Katrizky, *Tetrahedron*, **2000**, *56*, 1783.
14. Li, W. Q.; Tian, W. Q.; Feng, J. K.; Liu, Z. Z.; Ren, A. M.; Zhang, G. *J. Phys. Chem. A*, **2005**, *109*, 8391.
15. Li, X. W.; Pennington, W. T.; Robinson, G. H.; *J. Am. Chem. Soc.* **1995**, *117*, 7578.
16. Li, X. W.; Xie, Y.; Schreiner, P. R.; Gripper, K. D.; Crittendon, R. C.; Campana, C. F.; Schaefer, H. F.; Robinson, G. H.; *Organometallics*. **1996**, *15*, 3798.
17. Robinson, G. H. *Acc. Chem. Res.* **1999**, *32*, 773.
18. Ghiasi, R. *J. Mol. struc (THEOCHEM)*. **2005**, *718*, 225.
19. Ghiasi, R. *J. Organome. Chemistry*. **2005**, *690*, 4761.
20. Li, X.; Kuznetsov, A. E.; Zhang, H. F.; Boldyrev, A. I.; Wang, L. S. *Science*, **2001**, *291*, 859.
21. A. E. Kuznetsov, J. D. Corbett, L. S. Wang, A. I. Boldyrev, *Angew. Chem., Int. Ed.* **2001**, *40*, 3369.
22. Kuznetsov, A. E.; Boldyrev, A. I.; Li, X.; Wang, L. S. *J. Am. Chem. Soc.* **2001**, *123*, 8825.
23. Fowler, P. W.; Havenith, R. W. A.; Steiner, E. *Chem. Phys. Lett.* **2001**, *342*, 85.
24. Fowler, P. W.; Havenith, R. W. A.; Steiner, E. *Chem. Phys. Lett.* **2001**, *359*, 530.
25. Katrizky, A. R.; Barczynski, P.; Musumarra, G.; Pisano, D.; Szafran, M. *J. Am. Chem. Soc.* **1989**, *111*, 7.
26. Jug, K.; Koster, A. M. *J. Phys. Org. Chem.* **1991**, *4*, 163.
27. Schleyer, P. v. R.; Freeman, P. K.; Jiao, H.; Goldfuss, B., *Angew. Chem., Int. Ed. Engl.* **1995**, *34*, 337.
28. Bird, C. W. *Tetrahedron*, **1996**, *52*, 9945.
29. Schleyer, P. v. R.; Maerker, C.; Dransfeld, A.; Jiao, H.; Homm, N. v. E. *J. Am. Chem. Soc.* **1996**, *118*, 6317.
30. Schleyer, P. v. R.; Jiao, H.; *Pure Appl. Chem.* **1996**, *68*, 209.
31. Goldfuss, B.; Schleyer, P. v. R.; Hampel, F. *Organometallics*, **1996**, *15*, 1998.
32. Gaussian 98, Revision A.7, Frisch, M. J.; Trucks, G. W.; Schlegel, H. B.; Scuseria, G. E.; Robb, M. A.; Cheeseman, J. R.; Zakrzewski, V. G.; Montgomery, J. A.; Stratmann, J. R. E.; Burant, J. C.; Dapprich, S.; Millam, J. M.; Daniels, A. D.; Kudin, K. N.; Strain, M. C.; Farkas, O.; Tomasi, J.; Barone, V.; Cossi, M.; Cammi, R.; Mennucci, B.; Pomelli, C.; Adamo, C.; Clifford, S.; Ochterski, J.; Petersson, G. A.; Ayala, P. Y.; Cui, Q.; Morokuma, K.; Malick, D. K.; Rabuck, A. D.; Raghavachari, K.; Foresman, J. B.; Cioslowski, J.; Ortiz, J. V.; Baboul, A. G.; Stefanov, B. B.; Liu, G.; Liashenko, A.; Piskorz, P.; Komaromi, I.; Gomperts, R.; Martin, R. L.; Fox, D. J.; Keith, T.; Al-Laham, M. A.; Peng, C. Y.; Nanayakkara, A.; Gonzalez, C.; Challacombe, M.; Gill, P. M. W.; Johnson, B.; Chen, W.; Wong, M. E.; Andres, J. L.; Gonzalez, C.; Head-Gordon, M.; Replogle, E. S.; and Pople, J. A.; Gaussian, Inc., Pittsburgh PA, (1998).
33. Carpenter, J. E.; Weinhold, F. *J. Mol. Struct. (THEOCHEM)*. **1988**, *169*, 41.
34. (a) Becke, A. D.; *J. Chem. Phys.* **1993**, *98*, 5648.
35. Lee, C.; Yang, W.; Parr, R. G.; *Phys. Rev. B*. **1988**, *37*, 785.
36. Cheeseman, J. R.; Frisch, M. J.; Trucks, G. W.; Keith, T. A.; *J. Chem. Phys.* **1996**, *104*, 5497.
37. Keith, T. A.; Bader, R. F. *Chem. Phys. Lett.* **1993**, *210*, 223.
38. Li, Y. S.; Jalilian, M. R.; Durig, J. R. *J. Mol. Struct.* **1979**, *51*, 171.
39. Southern, J. F.; Schaefer, L.; Brendhaugen, K.; Seip, H. M. *J. Chem. Phys.* **1971**, *55*, 2418.
40. (a) Pearson, R. G.; *J. Org. Chem.* **1989**, *54*, 1423. (b) Zhou, Z.; Parr, R. G.; *Tetrahedron Lett.* **1988**, *29*, 4843. (c) Z. Zhou, R. G. Parr, *J. Am. Chem. Soc.* **1989**, *111*, 7371. (d) Minsky, A.; Meyer, A. Y.; Rabinovitz, M.; *Tetrahedron*, **1985**, *41*, 785. (e) Pearson, R. G.; *J. Am. Chem. Soc.* **1988**, *110*, 2092.
41. Pearson, R. G.; *Inorg. Chem.* **1988**, *27*, 734.
42. Reed, A. E.; Curtiss, L. A.; Weinhold, F.; *Chem. Rev.* **1988**, *88*, 899.